

# Impact of new measurements of light quarks at hadron colliders\*

Zihan Zhao (赵梓含)<sup>✉</sup> Minghui Liu (刘明辉)<sup>✉</sup> Liang Han (韩良)

School of Physical Sciences, University of Science and Technology of China, Hefei 230026, China

**Abstract:** Recently, a series of new measurements with both the neutral and charge current Drell–Yan processes have been performed at hadron colliders, revealing deviations from the predictions of the current parton distribution functions (PDFs). In this article, the impact of these new measurements is studied by using their results to update the PDFs. Although these new measurements correspond to different boson propagators and colliding energies, they are found to have a similar impact to the light quark parton distributions with a momentum fraction  $x$  of approximately 0.1. The deviations are consistent with each other and favor a larger valence  $d_v/u_v$  ratio than the modern PDF predictions. Further study indicates that such tension results dominantly from the deep inelastic scattering measurements of NMC and the fixed target experiments of NuSea, both of which play pivotal roles in detecting the relative  $u$ - and  $d$ -type quark contributions for modern PDFs. The conclusions of the impact study indicate that these new measurements should be included in the complete PDF global analysis in the future.

**Keywords:** Drell–Yan process, parton distribution functions, correlation study, data deviation

**DOI:** 10.1088/1674-1137/ae1186

**CSTR:** 32044.14.ChinesePhysicsC.50023107

## I. INTRODUCTION

The Drell–Yan processes [1], encompassing both neutral current  $hh(q_i\bar{q}_i) \rightarrow Z/\gamma^* \rightarrow \ell^+\ell^-$  and charged current  $hh(q_i\bar{q}_j) \rightarrow W^\pm \rightarrow \ell^\pm\nu$  production, constitute some of the most crucial inputs for proton parton distribution function (PDF) analyses. Within the framework of Quantum Chromodynamics (QCD), the Drell–Yan process is rigorously factorized [2] into a short-distance hard-scattering part calculable in perturbation theory and a universal long-distance non-perturbative part incorporated in the PDFs. This established factorization enables the Drell–Yan processes to serve as model-independent probes for PDF determination. At hadron colliders, the productions of Drell–Yan processes are primarily initiated by  $u$  ( $\bar{u}$ ) and  $d$  ( $\bar{d}$ ) quarks, which play a fundamental role in PDF studies. The colliding energy and kinematic features renders the Drell–Yan process sensitive to a wide range of the momentum fractions  $x$  of the initial-state quarks, particularly the region  $x \sim 0.1$ , where the so-called "valence" quarks  $u_v$  and  $d_v$  are strongly dominant. Furthermore, the Drell–Yan processes exhibit exceptional precision in both theoretical predictions and experimental measurements. Theoretically, the inclusive Drell–Yan production enables the resummation and fixed-order

perturbative QCD computations achieving percent-level accuracy. Experimentally, the final-state leptons originating from  $W/Z$  boson decays are detected with very high efficiencies and small uncertainties. Together with very small background contaminations, this enables experimental uncertainties to be well controlled at the percent level. Under these conditions, when new Drell–Yan measurements with high precision become available, their impacts on light quark PDFs should be examined. Deviations between data and predictions may imply potential limitations in current PDF models or QCD calculations. Such discrepancies offer unique opportunities to refine our understanding of proton structures.

Some recent Drell–Yan measurements, including the proton structure parameter  $R$  (closely approximating  $d_v/u_v$ ) [3] extracted from the forward–backward asymmetry ( $A_{FB}$ ) in  $Z/\gamma^* \rightarrow \ell^+\ell^-$  by the D0 [4] and CMS [5] collaborations, as well as the  $W$  charge asymmetry measurement at high transverse mass ( $m_T$ ) region by ATLAS [6], collectively reveal significant deviations from current PDF predictions in the parton momentum fraction range  $x \sim 0.1$ .

These new datasets exhibit distinctive characteristics. First, they can provide flavor-sensitive information about the relative contributions of  $u$  and  $d$  quarks. Although

Received 22 August 2025; Accepted 10 October 2025; Accepted manuscript online 11 October 2025

\* Supported by the National Natural Science Foundation of China (12061141005, 12105275)

<sup>✉</sup> E-mail: hepglmh@ustc.edu.cn



Content from this work may be used under the terms of the Creative Commons Attribution 3.0 licence. Any further distribution of this work must maintain attribution to the author(s) and the title of the work, journal citation and DOI. Article funded by SCOAP<sup>3</sup> and published under licence by Chinese Physical Society and the Institute of High Energy Physics of the Chinese Academy of Sciences and the Institute of Modern Physics of the Chinese Academy of Sciences and IOP Publishing Ltd

various Drell–Yan measurements [7–25] have been extensively incorporated into modern PDFs [26–28], direct experimental determination of the relative  $u$  and  $d$  quark distributions, such as the light quark ratio  $d/u$ , remains very rare. This difficulty arises because the Drell–Yan production occurs through both  $u\bar{u}$  and  $d\bar{d}$  initial states with comparable cross sections and identical final-state particles. Consequently, the  $u(\bar{u})$  and  $d(\bar{d})$  contributions are always mixed and experimentally indistinguishable, which makes the  $u$  and  $d$  quark determination heavily dependent on the choice of non-perturbative formalism in the global analysis. Second, with higher collider energies, the  $s$ -,  $c$ -, and  $b$ -type quark contributions become more significant, thereby complicating the dependence on non-perturbative assumptions in the PDF global fits. Fortunately, observables from these new datasets are deliberately designed to contain no or insignificant contributions from these heavy quarks. Owing to their significant deviations from PDF predictions, the distinctive features make the impact study of these new datasets on PDFs particularly crucial.

This study verifies whether deviations from all the three datasets are mutually consistent, which may indicate a coherent tendency in the  $u$  and  $d$  quark behaviors with respect to the current PDFs. The details are organized as follows: Section II presents a short review of the three new Drell–Yan measurements. Section III studies the correlations between these new measurements and the PDFs using the cosine of the Pearson correlation angle. Section IV examines the impact of these new measurements by updating the PDFs with their results. Section V presents a summary of the paper.

## II. REVIEW OF THE NEW DRELL–YAN MEASUREMENTS

For the neutral current Drell–Yan measurement, a recent method proposed in Ref. [3] enables a refined flavor decomposition through the forward-backward asymmetry ( $A_{FB}$ ) spectrum in the  $Z/\gamma^* \rightarrow \ell^+ \ell^-$  Drell–Yan process. The  $u$  ( $\bar{u}$ ) and  $d$  ( $\bar{d}$ ) quark information inside the  $A_{FB}$  observable can be factorized into a well-defined structure parameter,  $R$  [5], which serves as a novel experimental observable and reflects unique information regarding the relative difference between  $u$  and  $d$  quarks.

At a  $p\bar{p}$  collider such as the Tevatron and a  $pp$  collider such as the LHC, the observable  $R$  can be approximately expressed as

$$R_{p\bar{p}} \propto \frac{d(x_1)d(x_2) - \bar{d}(x_1)\bar{d}(x_2)}{u(x_1)u(x_2) - \bar{u}(x_1)\bar{u}(x_2)},$$

$$R_{pp} \propto \frac{d(x_1)\bar{d}(x_2) - \bar{d}(x_1)d(x_2)}{u(x_1)\bar{u}(x_2) - \bar{u}(x_1)u(x_2)}. \quad (1)$$

In the above definitions,  $x_{1,2}$  are the momentum fractions

of the two initial-state partons given by  $x_{1,2} = \frac{\sqrt{M^2+Q_T^2}}{\sqrt{s}} e^{\pm Y}$ , where  $M$ ,  $Y$ , and  $Q_T$  are the invariant mass, rapidity, and transverse momentum of the dilepton system in Drell–Yan productions, respectively, and  $\sqrt{s}$  is the collision center-of-mass energy. The convention  $x_1 > x_2$  is followed, reflecting the typical kinematic configuration at hadron colliders, where one parton carries a substantially larger momentum fraction than the other owing to the boost of the dilepton system. The contributions from  $s$ -,  $c$ -, and  $b$ -type quarks are nearly perfectly cancelled because of  $q(x, Q) = \bar{q}(x, Q)$ , for  $q = s$ ,  $c$ , and  $b$  up to the next-to-leading order (NLO) in QCD interactions, assuming an initial equality of approximately 1 GeV at  $Q_0$ . Given the approximation that the light-quark distributions are approximately flavor-symmetric at low  $x$  [26] (*i.e.*,  $u(x_2) \approx \bar{u}(x_2) \approx d(x_2) \approx \bar{d}(x_2)$  for  $x_2 \lesssim 5 \times 10^{-3}$ ), we can extract a ratio at both  $pp$  and  $p\bar{p}$  colliders:

$$R \propto \frac{d(x_1) - \bar{d}(x_1)}{u(x_1) - \bar{u}(x_1)} = \frac{d_v(x_1)}{u_v(x_1)}, \quad (2)$$

which provides a clean experimental probe of the valence quark ratio  $d_v/u_v$  in the  $x \sim 0.1$  region.

These analyses have been performed: one with the  $R$  parameter extracted using 1.96 TeV  $p\bar{p}$  collision data collected with the D0 detector at the Tevatron [4], and the other with the  $R$  parameter extracted using 8 TeV  $pp$  collision data collected with the CMS detector at the LHC [5]. Both results indicate an enhancement of the  $d_v/u_v$  ratio in the  $x$  region around 0.1 relative to the predictions from current PDF sets. These measurements are expected to provide unique information in the PDF analysis: the D0 measurement extracted the structure parameter  $R$  differentially in  $Z$  boson rapidity regions, focusing in particular on the interval  $1 < |Y| < 1.5$ , which corresponds to  $x_1 \sim 0.1$  and  $x_2 \sim 0.01$ . In this kinematic region, the measured  $R$  values were found to be significantly higher than the predictions of the three modern PDFs (CTEQ [26], MSHT [27] and NNPDF [28]) by more than 3.5 standard deviations, as illustrated in Fig. 1 (left panel). For the same observable extraction using CMS data in the forward rapidity intervals ( $1.25 < |Y| < 2.4$ ), corresponding to  $x_1 \sim 0.05–0.1$  and  $x_2 \sim 0.002$ , the measured  $R$  values were also found to be significantly larger than the predictions of the three PDFs, again implying an enhanced  $d_v/u_v$  ratio in the  $x \sim 0.1$  region (see Fig. 1, middle panel). Given the absence of direct constraints on the relative composition of valence quarks in current global PDF fits, such deviations are acceptable.

For the charged Drell–Yan process, ATLAS collaboration performed a  $W$  charge asymmetry ( $A_{ch}^W$ ) measurement in the high transverse mass region ( $m_T$  up to 5 TeV) at  $\sqrt{s} = 13$  TeV [6]. The  $W$  charge asymmetry is a classic experimental observable sensitive to the PDF, defined as

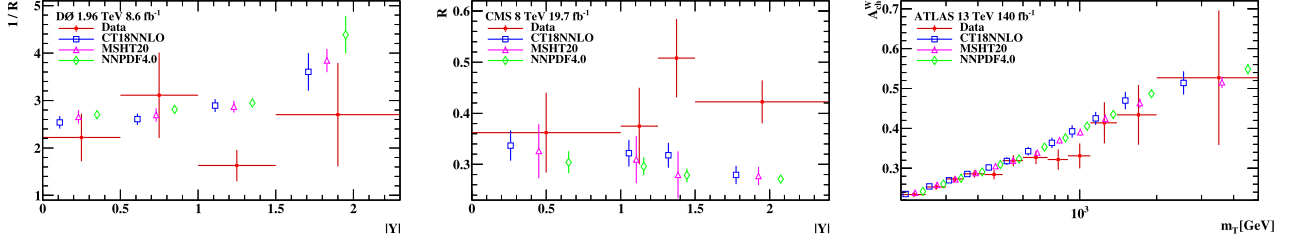


**Fig. 1.** (color online) Comparison between experimental measurements and theoretical predictions obtained using the modern PDF sets CT18NNLO [26], MSHT20 [27], and NNPDF4.0 [28], for observables sensitive to the flavor composition of the proton in hadron collider environments. The left panel shows the D0 measurement of the inverse  $1/R$  in the Drell–Yan process at  $\sqrt{s} = 1.96$  TeV, whereas the middle panel presents the CMS measurement of  $R$  at  $\sqrt{s} = 8$  TeV in a similar process. The right panel shows the ATLAS measurement of the  $W$  boson charge asymmetry  $A_{\text{ch}}^W$  at  $\sqrt{s} = 13$  TeV. According to Eq. (2),  $R$  is defined as a function of  $x_1$ , with  $x_1 \sim 0.1$  being a valid approximation only in the rapidity ranges  $1 < |Y| < 1.5$  for the D0 data and  $1.25 < |Y| < 2.4$  for the CMS data. The complete set of rapidity bins in the left (middle) panel covers a wider range of  $0.05 < x_1 < 0.4$  ( $0.005 < x_1 < 0.1$ ) values.

$A_{\text{ch}}^W = (\sigma_{W^+} - \sigma_{W^-})/(\sigma_{W^+} + \sigma_{W^-})$ , where  $\sigma$  is the measured cross sections. Compared with the traditional  $W$  charge asymmetry measurements, the high transverse mass requirement enables access to higher values of  $x$ , such as  $x \sim 0.1$ . In this  $x$  region, the initial  $u$  and  $d$  quarks lie very close to the valence peak distributions, whereas  $s(\bar{s})$ ,  $c(\bar{c})$ , and  $b(\bar{b})$  quarks reside in their tail parts. Consequently, the processes are overwhelmingly dominated by  $u$  and  $d$  quarks. This configuration serves as an independent probe for studying the relative  $d/u$  quark composition. Notably, a deficit is observed in the ATLAS results relative to the PDF prediction around  $m_r^W \sim 1$  TeV, suggesting that the relative structure of  $u$  and  $d$  quarks may differ from current PDF expectations (see Fig. 1, right panel). The corresponding  $x_1$  values probed in this high- $m_r^W$  region lie between 0.02 and 0.3, overlapping with the  $x_1$  range probed by the  $R$  measurements from both the D0 and CMS experiments.

Given that both observables, the high transverse mass region  $W$  charge asymmetry and  $R$  from  $A_{FB}$ , can provide information on the relative  $u$  and  $d$  quark contributions and show deviations from current PDF predictions, particularly considering that these measurements are performed at different colliders with different center-of-mass energies, involving different processes and distinct production mechanisms for accessing the  $x \sim 0.1$  region, their mutual consistency is particularly interesting. As there are two quarks in the initial states,  $q(x_1)\bar{q}^{(\prime)}(x_2)$  and  $\bar{q}^{(\prime)}(x_1)q(x_2)$  are always mixed, we must quantitatively investigate the correlations among these datasets and their collective impact on the  $u$  and  $d$  quark PDFs of the proton.

### III. DATASET PDF CORRELATION PATTERNS AND IMPLICATIONS

A commonly used approach to examine the relative correlation and mutual compatibility of the experimental datasets is to compute the cosine of the Pearson correla-

tion angle  $C_H(X, Y)$  [29] between two quantities  $X$  and  $Y$ . In the multidimensional parameter space of the Hessian PDF framework [30–32], this evaluation is performed by computing the variations in  $X$  and  $Y$  under unit displacements along each eigenvector direction  $k$  of the PDF error set. Specifically,  $X_{\pm k} \equiv X(0, \dots, \pm 1, \dots, 0)$  and  $Y_{\pm k}$  denote the values of  $X$  and  $Y$  evaluated at the  $\pm 1\sigma$  positions along the  $k$ -th eigenvector direction. The uncertainties  $\delta_H X$  and  $\delta_H Y$  are defined as  $\delta_H X = \frac{1}{2} \sqrt{\sum_{k=1}^D (X_{+k} - X_{-k})^2}$  and  $\delta_H Y = \frac{1}{2} \sqrt{\sum_{k=1}^D (Y_{+k} - Y_{-k})^2}$ . The correlation angle is then computed as

$$C_H(X, Y) = \frac{1}{4\delta_H X \delta_H Y} \sum_{k=1}^D (X_{+k} - X_{-k})(Y_{+k} - Y_{-k}) = \frac{\sum_{k=1}^D (X_{+k} - X_{-k})(Y_{+k} - Y_{-k})}{\sqrt{\sum_{k=1}^D (X_{+k} - X_{-k})^2} \sqrt{\sum_{k=1}^D (Y_{+k} - Y_{-k})^2}}. \quad (3)$$

Under this convention, the cosine of the correlation angle between the minimal fit  $\chi^2$  for dataset  $E$  and parton distribution function  $f$  is defined as

$$C_H(E, f) = \frac{\sum_{k=1}^D (\chi^2_{E(+k)} - \chi^2_{E(-k)})(f_{+k} - f_{-k})}{\sqrt{\sum_{k=1}^D (\chi^2_{E(+k)} - \chi^2_{E(-k)})^2} \sqrt{\sum_{k=1}^D (f_{+k} - f_{-k})^2}} \quad (4)$$

Thus, a positive  $C_H(E, f)$  value generally implies that the direction minimizing  $\chi^2_E$  simultaneously reduces the value of PDF  $f$ . Conversely, a negative  $C_H(E, f)$  indicates that dataset  $E$  preferentially enhances  $f$ .

Since  $\chi^2_E$  depends on the theoretical predictions for the observables in dataset  $E$ , the RESBOS generator [33] is employed for neutral Drell–Yan process predictions, and MCFM [34] is employed for charged Drell–Yan process predictions. RESBOS provides approximate NNLO QCD +  $N^3LL$  resummation and electroweak corrections via the effective Born approximation [35]. The MCFM program

provides NNLO QCD predictions for W-boson production, incorporating NLO electroweak corrections.

To identify which parton distribution functions are primarily responsible for the potential deviations observed among the three datasets, and to assess the consistency of their  $x$ -dependent correlation patterns, we show the  $C_H(E, f)$  between the new datasets and the  $u_v$ ,  $d_v$ ,  $d_v/u_v$ ,  $u$ ,  $d$ ,  $d/u$ ,  $\bar{u}$ ,  $\bar{d}$ , and  $\bar{d}/\bar{u}$  PDFs in Fig. 2. The quark PDFs are obtained from CT18NNLO. The D0 1.96 TeV  $R$  measurement (blue curve), CMS 8 TeV  $R$  measurement (green curve), and ATLAS 13 TeV  $A_{ch}^W$  measurement (pink curve) are plotted together. Note that the exact definition of  $R$ , as given in Ref. [5], is employed in this section and Section IV, rather than the approximate expressions presented in Eqs. (1) and (2).

Very similar patterns of behavior are observed among the different  $C_H(E, f)$  distributions in Fig. 2, reflecting the common physical sensitivity of the three new measurements. For the valence  $u$  quark PDF ( $u_v$ , top-left panel), all three datasets yield positive  $C_H(E, f)$  values in the  $x$  region around 0.1, corresponding to the larger- $x$  parton in their kinematics. From the definition of  $C_H$ , a positive correlation generally indicates that minimizing  $\chi_E^2$  for a given dataset is accompanied by a reduction in the value of  $f_{u_v}$  in this region. This consistent trend implies that all three measurements favor a lower  $u_v$  compared with the CT18NNLO prediction at  $x \sim 0.1$ , corresponding with the

observed excess of  $R$  and the deficit in  $A_{ch}^W$  discussed in Section II. A complementary pattern is observed for the valence  $d$  quark PDF ( $d_v$ , top-middle panel), where all datasets exhibit negative  $C_H(E, f)$  values in the same  $x$  region. This generally indicates that these datasets tend to enhance  $d_v$  in this region, together with a reduction in  $u_v$ , implying that the deviations in  $R$  and  $A_{ch}^W$  can be jointly interpreted as a preference for a larger  $d_v/u_v$  ratio than modern PDF predictions, in agreement with the negative value of the valence  $d$ -to- $u$  ratio ( $d_v/u_v$ , top-right panel) at  $x \sim 0.1$ .

The middle-row panels show the correlations with the  $u$ ,  $d$ , and  $d/u$  PDFs. At  $x \sim 0.1$ ,  $u$  exhibits a positive correlation for all datasets, again indicating a preference for a downward shift in this range, whereas  $d$  exhibits the opposite sign, indicating an enhanced  $d$  quark density. These patterns persist for the antiquark PDFs ( $\bar{u}$ ,  $\bar{d}$ , and  $\bar{d}/\bar{u}$ , bottom panels), where  $\bar{d}$  follows the same trend as  $u$ , and  $\bar{u}$  follows the same trend as  $d$  at  $x \sim 0.1$ . Consequently, these behaviors lead to a negative value of  $d/u$  and a positive value of  $\bar{d}/\bar{u}$  at  $x \sim 0.1$ , thereby reinforcing the conclusion that the observed deviations in  $R$  and  $A_{ch}^W$  can be simultaneously accounted for by a shift in the valence-quark ratio  $d_v/u_v$ , defined as  $(d - \bar{d})/(u - \bar{u})$ .

In summary, the strong correlation patterns for  $u_v$ ,  $d_v$ , and  $d_v/u_v$ , together with the consistent behavior in the  $u$ ,  $d$ ,  $d/u$ ,  $\bar{u}$ ,  $\bar{d}$ , and  $\bar{d}/\bar{u}$  PDFs, provide quantitative evid-

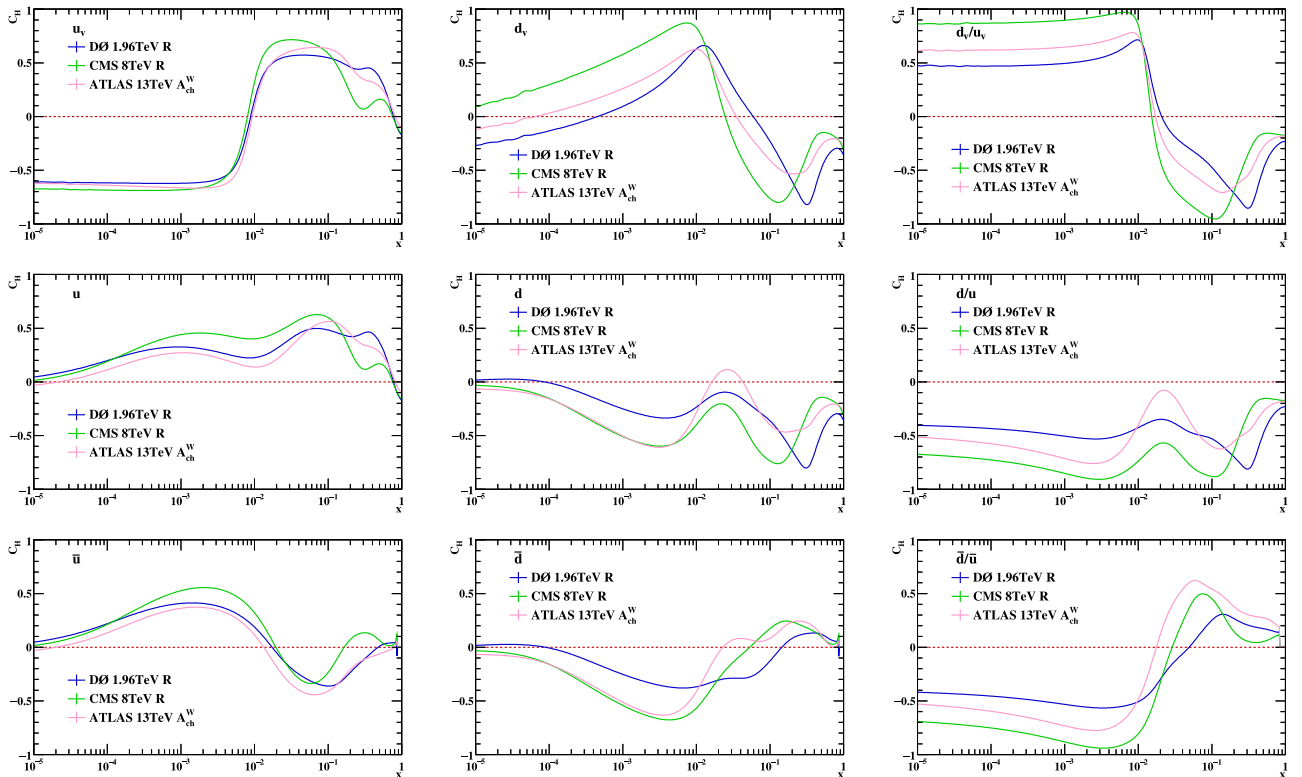


**Fig. 2.** (color online)  $C_H(E, f_{\text{parton}})$  (parton =  $u_v$ ,  $d_v$ ,  $d_v/u_v$ ,  $u$ ,  $d$ ,  $d/u$ ,  $\bar{u}$ ,  $\bar{d}$ , and  $\bar{d}/\bar{u}$ , respectively) as a function of  $x$ , showing the correlation between each dataset and the parton PDF  $f_{\text{parton}}$  from CT18NNLO.

ence that the three new datasets are pulling the current PDFs in the same direction of increasing  $d_v/u_v$  ratio at  $x \sim 0.1$ . This mutual agreement supports the conclusion that the observed deviations are unlikely to be independent statistical fluctuations but rather reflect a coherent deviation with the central predictions of current PDFs.

#### IV. COMPATIBILITY AND TENSION ANALYSIS VIA WEIGHTED PDF UPDATING

To further assess the compatibility between the three new hadron collider measurements and the datasets currently input to modern global PDF fits, as well as to investigate their impact on the PDF updating results, we employ the error PDF updating method package (**ePUMP**) [30, 36] to update the CT18NNLO [26] PDFs. **ePUMP** facilitates efficient updating of the best-fit PDF set and Hessian eigenvector pairs of PDF sets (*i.e.*, error PDFs) in terms of new data by retaining all theoretical assumptions of the original global fit, such as the choice of parametrization and number of parameters. In Ref. [36], the **ePUMP** framework is validated through detailed comparisons with full global analyses, and its potential is illustrated via selected phenomenological applications relevant to the LHC. In this work, the probed  $x$  regions and related energy scale  $Q$  regions lie within the validated applicability range of Ref. [36]. Therefore, despite the fixed assumptions, the qualitative conclusions regarding the impact of the new measurements remain valid.

The PDF updating is performed by systematically varying the statistical weights of the three newly input datasets ( $R_{D0}$ ,  $R_{CMS}$ , and  $A_{ch,ATLAS}^W$ ) from 0 to 15, thereby progressively enhancing their influences in the PDF updating process. This procedure enables an assessment of how the global fit responds and whether these measurements are consistent or in tension with the existing inputs. Among the pre-existing datasets included in the modern PDFs, the NMC [22] and NuSea [24] datasets exhibit the most significant tensions with the three new hadron collider Drell–Yan measurements and are therefore highlighted. The NMC dataset provides values of the structure function ratio  $F_2^D/F_2^p$  extracted from deep inelastic muon scattering on hydrogen ( $p$ ) and deuterium ( $D$ ), which is sensitive to the relative flavor composition of  $u$  and  $d$  quarks. The NuSea dataset is a Drell–Yan dimuon measurement with proton and deuteron targets, providing direct access to the  $\bar{d}/\bar{u}$  ratio through the comparison of  $pp$  and  $pD$  cross sections, and reporting a pronounced enhancement of the  $\bar{d}/\bar{u}$  distribution.

As shown in Fig. 3, the shifts in the updating are quantified by evaluating the changes in  $\chi^2$  for selected datasets, expressed as  $\Delta\chi^2 = \chi^2_{\text{original PDF}} - \chi^2_{\text{updated PDF}}$ . In this representation, an increasing  $\Delta\chi^2$  curve indicates that the selected dataset favors PDF modifications in the same direction as the three new data inputs, whereas a de-

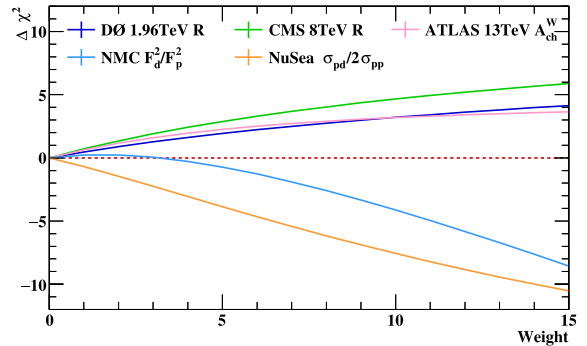


**Fig. 3.** (color online) Impact on the global fit by increasing the weight (from 0 to 15) of the three new input datasets ( $R_{D0}$ ,  $R_{CMS}$ ,  $A_{ch,ATLAS}^W$ ). The effect is quantified by the changes in  $\chi^2$  for the five selected datasets. Each curve shows  $\Delta\chi^2 = \chi^2(E)_{\text{original PDF}} - \chi^2(E)_{\text{updated PDF}}$  as a function of the updating weight applied to the corresponding dataset. An increasing slope reflects aligned PDF preferences, whereas a decreasing slope indicates opposite tendencies and potential tension.

ing trend suggests a tension. The three new hadron collider Drell–Yan datasets exhibit monotonically increasing trends, indicating a consistent preference for the updated PDFs. By contrast, the NMC and NuSea datasets show generally decreasing curves with larger  $\chi^2_{\text{updated PDF}}$  values, highlighting a significant tension between these fixed-target measurements and the new hadron collider Drell–Yan data.

To further illustrate the impact of the three new datasets on individual parton densities, we compare the original CT18NNLO PDF set with the updated version generated through the **ePUMP** tool, where each dataset was assigned a weight of 15. Figure 4 shows the ratios of the updated PDFs to the original ones, together with their uncertainties, for nine selected parton flavors:  $u_v$ ,  $d_v$ ,  $d_v/u_v$ ,  $u$ ,  $d$ ,  $d/u$ ,  $\bar{u}$ ,  $\bar{d}$  and  $\bar{d}/\bar{u}$ , all evaluated at  $Q = 100$  GeV.

The most pronounced changes appear in the valence quark PDFs within the  $x \sim 0.1$  region, where all three datasets have their strongest sensitivity. Consistent with the  $C_H(E, f)$  correlation patterns in Fig. 2, the updated  $u_v$  distribution exhibits a downward shift in this range, whereas  $d_v$  shows a corresponding enhancement, jointly indicating a preference for a larger  $d_v/u_v$  ratio. The same flavor-dependent tendency is also visible in the other quark PDFs:  $u$ ,  $\bar{d}$ , and  $\bar{d}/\bar{u}$  are reduced, whereas  $d$ ,  $\bar{u}$ , and  $d/u$  are enhanced, in agreement with the correlation analysis discussed in Section III. Outside the  $x \sim 0.1$  region, the observed shifts are largely driven by the valence quark sum rules  $\int_0^1 u_v(x)dx = 2$  and  $\int_0^1 d_v(x)dx = 1$ .

#### V. SUMMARY

Recent hadron collider Drell–Yan measurements including the  $R$  ratios from forward-backward asymmetry

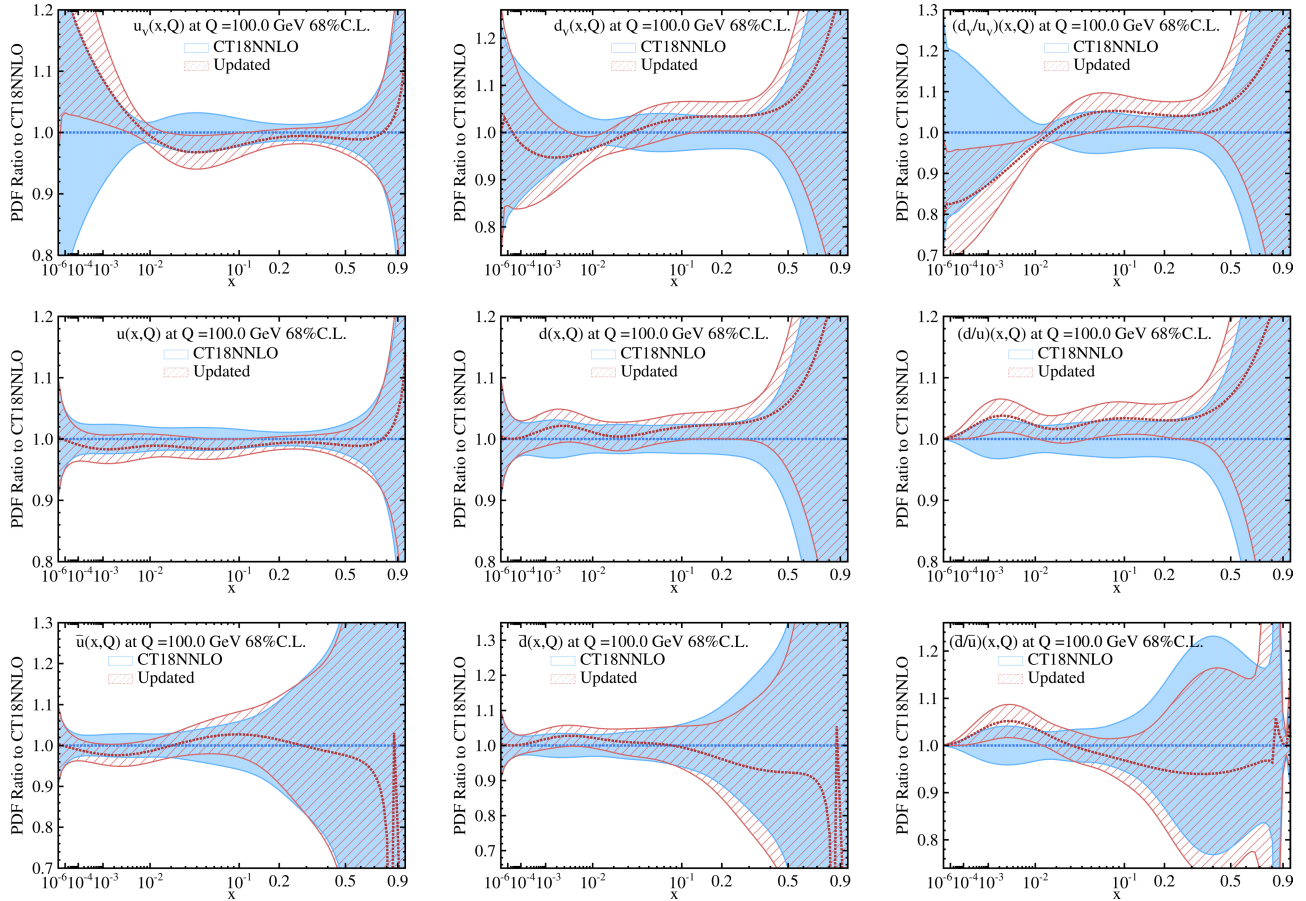


**Fig. 4.** (color online) Comparison between updated PDFs, which are updated using the three new datasets with a weight of 15, and the original CT18NNLO central predictions. Each plot shows the ratio of the updated PDF to the original one, with associated uncertainty bands.

at D0 and CMS, and the high- $m_T$   $W$  charge asymmetry  $A_{\text{ch}}^W$  from ATLAS, exhibit a coherent preference for an enhanced  $d_v/u_v$  ratio in the  $x \sim 0.1$  region. Despite the differences in collider types, energies, and observables, these measurements demonstrate strong mutual consistency, particularly in their correlation patterns within the global fit parameter space. A clear tension is observed between these collider measurements and fixed-target datasets such as NMC and NuSea, which have traditionally played a dominant role in constraining the relative

light quark flavor structure. This result indicates a distinct trend in the preferred flavor composition of  $u$  and  $d$  quarks. Future measurements with higher statistics will be crucial for placing more stringent constraints on the light-quark compositions. Note that in this study, the results are derived from the ePUMP analysis tool, and the associated momentum fraction  $x$  represents only a Leading Order approximation. Therefore, a full PDF global analysis is required for more robust conclusions.

## References

- [1] S. D. Drell and T. M. Yan, *Phys. Rev. Lett.* **25**, 316 (1970)
- [2] J. C. Collins, D. E. Soper, and G. Sterman, arXiv: [hep-ph/0409313](https://arxiv.org/abs/hep-ph/0409313)
- [3] S. Yang *et al.*, *Phys. Rev. D* **106**, 033001 (2022)
- [4] V. M. Abazov *et al.* (D0 Collaboration), *Phys. Rev. D* **110**, L091101 (2024)
- [5] M. Xie, S. Yang, W. Ma *et al.*, arXiv: [2505.17608](https://arxiv.org/abs/2505.17608)
- [6] M. Aaboud *et al.* (ATLAS Collaboration), *JHEP* **07**, 026 (2025)
- [7] H. Abramowicz *et al.* (H1, ZEUS Collaborations), *Eur. Phys. J. C* **75**, 580 (2015)
- [8] V. Abazov *et al.* (D0 Collaboration), *Phys. Rev. D* **76**, 012003 (2007)
- [9] T. A. Aaltonen *et al.* (CDF Collaboration), *Phys. Lett. B* **92**, 232 (2010)
- [10] R. Aaij *et al.* (LHCb Collaboration), *JHEP* **08**, 039 (2015)
- [11] R. Aaij *et al.* (LHCb Collaboration), *JHEP* **05**, 109 (2015)
- [12] M. Aaboud *et al.* (ATLAS Collaboration), *Eur. Phys. J. C* **77**, 367 (2017)
- [13] G. Aad *et al.* (ATLAS Collaboration), *Eur. Phys. J. C* **76**, 291 (2016)

[14] D. Acosta *et al.* (CDF Collaboration), *Phys. Rev. D* **71**, 051104 (2005)

[15] V. M. Abazov *et al.* (D0 Collaboration), *Phys. Rev. D* **77**, 011106 (2008)

[16] S. Chatrchyan *et al.* (CMS Collaboration), *Phys. Rev. Lett.* **109**, 111806 (2012)

[17] G. Aad *et al.* (ATLAS Collaboration), *Phys. Rev. D* **85**, 072004 (2012)

[18] V. M. Abazov *et al.* (D0 Collaboration), *Phys. Rev. D* **91**, 032007 (2015); **91**: 079901(E) (2015)

[19] V. Khachatryan *et al.* (CMS Collaboration), *Eur. Phys. J. C* **76**, 469 (2016)

[20] A. C. Benvenuti *et al.* (BCDMS Collaboration), *Phys. Lett. B* **223**, 485 (1989)

[21] A. C. Benvenuti *et al.* (BCDMS Collaboration), *Phys. Lett. B* **237**, 592 (1990)

[22] M. Arneodo *et al.* (New Muon Collaboration), *Nucl. Phys. B* **483**, 3 (1997)

[23] G. Moreno, C. N. Brown, W. E. Cooper *et al.*, *Phys. Rev. D* **43**, 2815 (1991)

[24] R. S. Towell *et al.* (NuSea Collaboration), *Phys. Rev. D* **64**, 052002 (2001)

[25] J. C. Webb *et al.* (NuSea Collaboration), *Nucl. Phys. A* **721**, 344 (2003)

[26] T.-J. Hou, J. Gao, T. J. Hobbs *et al.*, *Phys. Rev. D* **103**, 014013 (2021)

[27] S. Bailey, T. Cridge, L. A. Harland-Lang *et al.*, *Eur. Phys. J. C* **81**, 341 (2021)

[28] R. D. Ball *et al.* (NNPDF Collaboration), *Eur. Phys. J. C* **82**, 428 (2022)

[29] J. Pumplin, D. Stump, R. Brock *et al.*, *Phys. Rev. D* **65**, 014013 (2001)

[30] C. Schmidt, J. Pumplin, C. P. Yuan *et al.*, *Phys. Rev. D* **98**, 094005 (2018)

[31] H. Paukkunen and P. Zurita, *JHEP* **12**, 100 (2014)

[32] S. Camarda *et al.* (xFitter Collaboration), *Eur. Phys. J. C* **75**, 458 (2015)

[33] C. Balazs and C. P. Yuan, *Phys. Rev. D* **56**, 5558 (1997)

[34] R. Boughezal, J.M. Campbell, R.K. Ellis *et al.*, *Eur. Phys. J. C* **77**, 7 (2017)

[35] P. A. Zyla *et al.* (Particle Data Group), *Prog. Theor. Exp. Phys.* **2020**, 083C01 (2020)

[36] T.-J. Hou, Z.T. Yu, S. Dulat *et al.*, *Phys. Rev. D* **100**, 114024 (2019)